small
www.small-journal.com

Microsphere-Assisted Robust Epidermal Strain Gauge for Static and Dynamic Gesture Recognition

*Zongming Su, Haotian Chen, Yu Song, Xiaoliang Cheng, Xuexian Chen, Hang Guo, Liming Miao, and Haixia Zhang**

A novel and robust epidermal strain gauge by using 3D microsphere arrays to immobilize, connect, and protect a multiwalled carbon nanotubes (MWNTs) pathway is presented. During the solvent deposition process, MWNTs sedimentate, self-assemble, and wrap onto surface of polystyrene (PS) microspheres to construct conductive networks, which further obtain excellent stretchability of 100% by combining with commercially used elastomer. Benefiting from its 3D conductive pathway defined by microspheres, immobilized MWNT (I-MWNT) network can be directly used in practical occasions without further packaging and is proved by tape tests to be capable of defend mechanical damage effectively from external environment. By parameter optimization, the strain sensor with 3 μm PS spheres obtains stable resistive responses for more than 1000 times, and maintains its gauge factor (GF) of 1.35. This thin-film conductive membrane built by this effective construction method can be easily attached onto fingers of both robot and human, and is demonstrated in sensitive epidermal strain sensing and recognizing different hand gestures effectively, in static and dynamic modes, respectively.

1. Introduction

Highly flexible and stretchable electronic materials can easily be attached onto clothes or directly onto human body, and their possible applications include the detection of human motion, monitoring health and therapeutics. The basic issue of stretchable electronics focuses on material selection,[1,2] conductive path construction,[3] and corresponding reliability[4,5] of the device. For every electronic device, electrode is regarded as the crucial part in process of signal generation, transmission, and detection. The properties of electrodes, such as conductivity and reliability, are important for stretchable electronics (e.g., e-skin,[6] stretchable light-emitting device,[7] and stretchable actuators[8]). The most important property of the stretchable electronics is its strain tolerance. However, the conventional strain sensor, mainly based on the brittle materials, typically suffers from low stretchability (maximum strain of 5%), which can hardly be used on human body with maximum strain of 40%.[9] There are increasing demands for thin-film strain sensor with large strain tolerance for epidermal applications.[6,10–12]

There are two mainstream strategies to construct stretchable conductive materials. The first one is to design different geometric patterns to introduce stretchability into intrinsically brittle and non-stretchable materials, e.g., metal membrane.[13] For example, cracks have been utilized for discontinuous structures patterned at different length scales when they are stretched.[14] Buckling of conductive materials by depositing a high-modulus thin film onto a prestrained elastomeric substrate resulting in the formation of buckled films after relaxation of the membrane,[15,16] is another common approach.

The second strategy adopts percolation conductive nanomaterial networks,[17–20] as they can maintain conductance as well as flexibility and stretchability under bending and stretching manipulation when integrated with elastomer substrates. Metal nanowire percolation networks (e.g., silver nanowire) are actively studied[19,21] as a highly stretchable electrode and strain sensor materials, even with some unneglectable drawbacks of high price or low chemical stability. Carbon nanotubes (CNTs),[22] remarked for their exceptional electronic and mechanical properties, chemical stability, as well as low cost, have also been widely used. Solution deposition techniques, including vacuum filtration,[23] spin-coating,[24] spray-coating,[25] and inkjet printing,[26] are basic fabrication methods. However, due to its feature of surface deposition, the conductive pathway promoted by solution deposition techniques, e.g., spray coating, cannot be directly used without further packaging, because the absorbed CNTs on surface of elastomers are only fixed by intermolecular force,[23,24] which is not strong enough to resist damage from external environment. An alternative protection of sealing CNT networks by another layer of elastomer may increase process complexity and membrane thickness, while causing current lead difficulties.[27]

Z. Su, Y. Song, X. Cheng, L. Miao, Prof. H. Zhang
Institute of Microelectronics
Peking University
Beijing 100871, China
E-mail: zhang-alice@pku.edu.cn
H. Chen, X. Chen, H. Guo
Academy for Advanced Interdisciplinary Studies
Peking University
Beijing 100871, China

DOI: 10.1002/smll.201702108

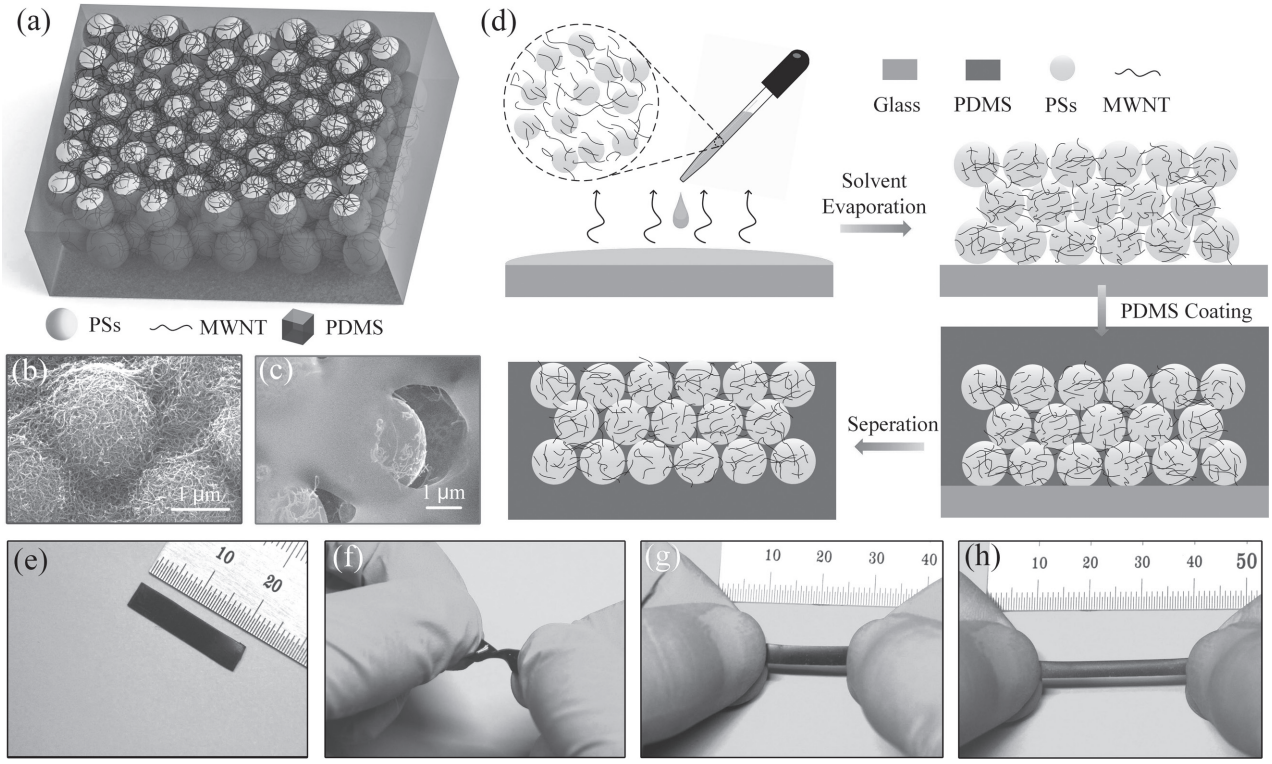

Figure 1. a) Schematic diagram of immobilized MWNT (I-MWNT) networks strain sensor. b) SEM image of wrapped MWNTs on PS sphere (PSs) array. c) SEM image of MWNT/PSs/PDMS composite. d) Fabrication process of stretchable I-MWNT network membrane. Optical images of e) conductive membrane, f) twisted by hand, g) stretched from original state to h) 100% elongation.

In this paper, we promote a new method to fabricate highly robust and stretchable multiwalled carbon nanotubes (MWNT) networks for epidermal strain gauge, which can be directly used without further packaging. Three different materials are mainly included: MWNT, polystyrene (PS) microsphere, and polydimethylsiloxane (PDMS). MWNTs work as the conductive nanomaterial, while PDMS provides stretchability for the conductive pathway. PS sphere (PSs) arrays, which assist MWNTs build 3D structures by capillarity during solvent evaporation, function as matrix and preserver for MWNT networks. The as-fabricated immobilized MWNT (I-MWNT) conductive membrane can be stretched to 100% with regular resistive response even after 1000 times of tests. When compared with the sprayed CNT networks on flat PDMS in the tape test, the membrane has barely resistance changes and proves robust reliability. Furthermore, the strain gauges have been demonstrated for static and dynamic human motion detection and can recognize different finger gestures in our experiments.

2. Results and Discussion

2.1. Fabrication and Characterization

The microsphere arrays help fixing and protecting conductive materials, because MWNTs can easily wrap onto PS microspheres after self-assembled process during solvent evaporation.[28] In this way to construct conductive pathway shown in **Figure 1**, MWNTs absorb on microsphere array surface, connect to each other, and build up to 3D structures. With conductive 3D structures only by MWNTs and PS microsphere arrays (MWNT/PSs), the membrane cannot be stretched. PDMS, the common used stretchable elastomer with large yield strength, has been used for stretchable electrode fabrication. It surrounds MWNTs and PS microsphere arrays altogether and solidified as the substrate of the strain gauge.

Scanning electron microscope (SEM) images of samples in different fabrication process are shown in Figure 1b,c. Figure 1b shows the as-fabricated MWNTs/PS microspheres composites, which illustrates the dense cover of MWNTs on PS microspheres array and proves the tight connection between them. After the introduction of PDMS, the MWNTs/PS microspheres composites are entirely wrapped by stretchable substrate. Figure 1c shows the conductive MWNTs/PSs/PDMS composites, in which the wrapped MWNTs can be observed on PS sphere and in PDMS matrix. The SEM images of cross section view can be referred in Figure S1 in the Supporting Information.

The fabrication process shown in Figure 1d is mainly based on solution deposition method and benefits from its mass productive and cost-effective advantages. In general, the fabrication processes include the following four steps: first, dip-coating MWNT/PS microspheres suspension onto substrate; second, evaporation of solvent and sedimentation of micro/nanocomposites; third, introduction of liquid PDMS into MWNTs/PS microspheres matrix by negative pressure

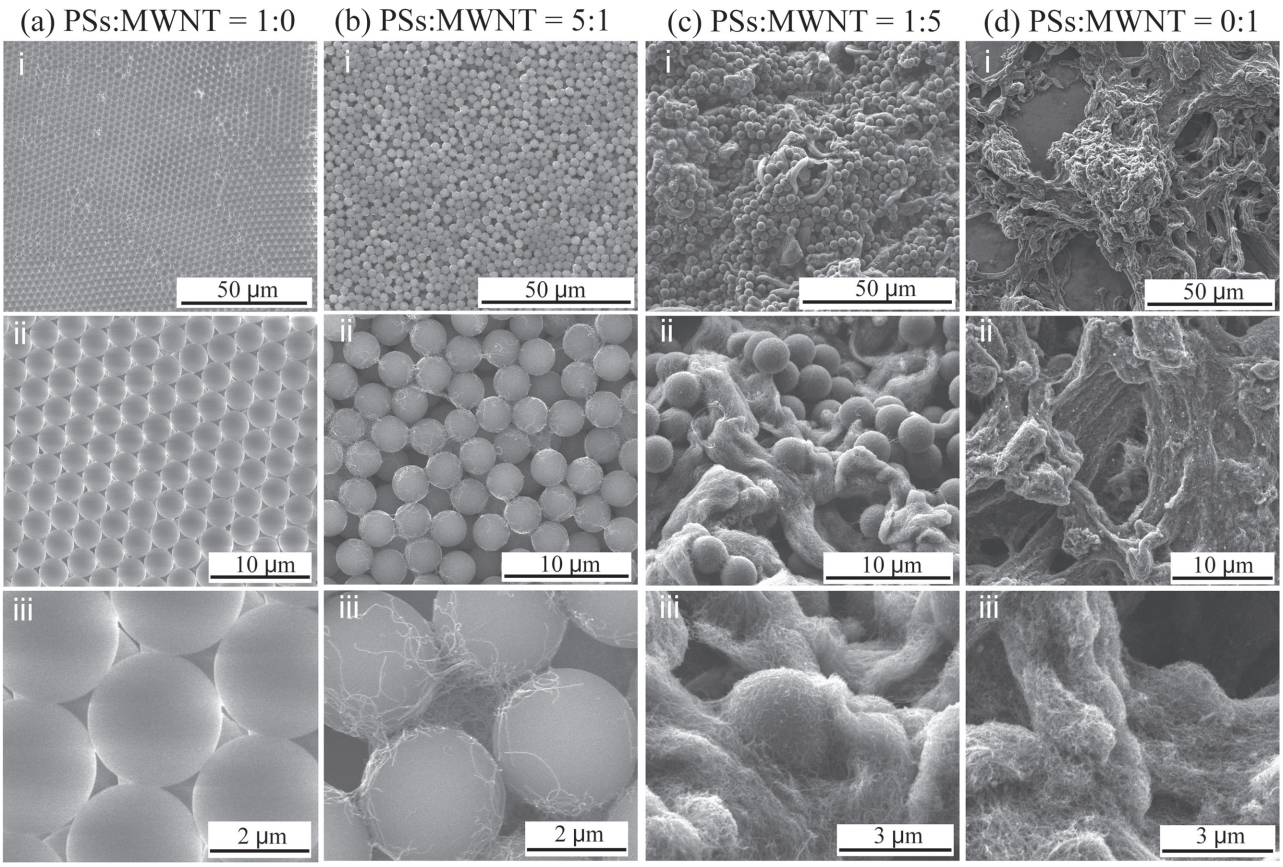

Figure 2. Recipe control for I-MWNT networks' fabrication. a) SEM images of sample without MWNT. PSs self-assemble to perfect HCP packaging. b) SEM images of sample with a ratio of 5:1 (PSs:MWNT). MWNT wraps to surface of PSs array and slightly interrupt the self-assembly process of PSs. c) SEM images of sample with a ratio of 1:5 (PSs:MWNT). The composite has too many MWNTs, which assemble and wrap PSs as MWNT clusters. d) SEM images of sample without PSs. MWNTs assemble to irregular clusters and unable to cover the whole surface of substrate without the assistance of self-assembly of PSs. Sub-panels (i), (ii), and (iii) show different sizes of view for each recipe.

method; at last, solidification process of PDMS and entire separation from substrate. With these four simple steps, the stretchable immobilized MWNT membrane can be fabricated on glass substrate. The detailed parameters and the fabrication process are shown in the Experimental Section. Further treatments like incision can help to prepare different shapes of conductive membrane as wished.

With conductive layer of MWNTs/PS microspheres on one side of the membrane, the membrane appears to be rough and black at that side, while smooth and transparent on the other side. Photographs of the samples are shown in Figure 1e. The membrane exhibits excellent flexibility and stretchability during simple manipulation by hands. Figure 1f shows highly twisted sample by hands. Meanwhile, it is stretched to maximum 100%, which is shown in Figure 1g,h.

2.2. Experimental Parameters Analysis

Different parameters in fabrication process can be controlled and adjusted for different purposes. Generally, the amount of MWNTs added into the mixed suspension decides the conductance of the membrane because of the increased conductive materials. The thickness of the conductive network relies on the amount of PS microspheres, while the thickness of the whole strain gauge can be adjusted by the quantity of PDMS. The mechanical property is determined by PDMS recipe (ratio of elastomer and cross-linker) and the solidification parameters, e.g., temperature.

There are two main issues need to be discussed related to PS microsphere. The first is the existence of PSs, which means how PSs help construct conductive networks and what if it does not exist. The results based on a series of experiments are shown in **Figure 2**, in which the ratio of PSs and MWNT (see the Experimental Section for detailed definition) changes from 1:0, 5:1, 1:5, and 0:1 and other experimental parameters are controlled (3 μm PSs). Figure 2a shows nearly perfect hexagonal closed-packed (HCP) array for PSs, which is insulating. With the introduction of MWNTs, the conductive pathway is constructed while HCP array is disturbed. When the amount of MWNT is low, relative regular array can be observed in Figure 2bi, as well as a small amount of MWNTs wrapped around PSs (Figure 2biii). When the amount of MWNT is very high, MWNTs can easily assemble to clusters themselves, while limited amount of PS spheres is embedded in MWNT clusters (Figure 2c). In this case, the conductive network is not dense enough to cover every

inch of the substrate, which means it is not continuous (see optical image in Figure S2 in the Supporting Information). This phenomenon becomes more prominent when there is no PSs added in the recipe (Figure 2d). MWNT assembles to very large clusters and leaves quite large areas empty, as can be observed in Figure 2di. There are two main disadvantages for the MWNT clusters: first, it leads to mechanical and electrical inhomogeneity in its first place; second, the highly dense MWNT clusters prevent liquid PDMS from permeation inside and lead to fabrication failure for MWNT/PDMS composite by this method.

The second issue need to be discussed is the size of PS spheres. In our experiments, 1, 3, and 5 μm PSs have been used (PSs:MWNT = 1:1), and the results are shown in **Figure 3**. For all these three sizes, MWNTs can effectively wrap onto surface of PSs. The moderate PSs and MWNT ratio ensure dense cover on surface of PSs (Figure 3ai–ci), continuity on glass substrate, and appropriate electrical resistance. A difficulty, however, has been found when 1 μm PSs is used to fabricate MWNT/PSs/PDMS composite (see Figure S3 in the Supporting Information). To be exact, the separation process in the fabrication flow is failed. After MWNT/PSs composites are fabricated, the 3D framework of the composite is completely defined. Liquid PDMS is then added to fill the remaining space defined by MWNT/PSs composite. If the size of PSs is small, the thin PDMS tunnels restricted by size effect of PSs tend to break during separation process, which means MWNT/PSs/PDMS composites are left onto glass surface. A reasonable conclusion is that PSs smaller than 1 μm is also difficult for separation because of the same reason. However, this effect can be eliminated when the size of PSs increases to 3 μm. Till now, the PSs has revealed its two different effects: assists the assembly process by capillarity and defines 3D framework by its size.

After successful separation process, the surface morphology of MWNT/PSs/PDMS can be observed by SEM and shown in Figure 3d. In the magnified view in Figure 3diii, the exposed MWNTs from the surface of PDMS act as the conductive dots for current lead. This specific morphology explains two important things. First, we do not need to package the membrane for practical applications as the conductive pathway has already been protected from external damage by PDMS. Second, the electrical current can be effectively conducted out by MWNT dots on its surface.

2.3. Resistive Response Test

I-MWNT networks have a representative feature of composite films which utilize a percolation-based conduction mechanism.[20,29] **Figure 4**a shows the schematic of conductive nanotubes network in elastomer matrix. In microstructural point of

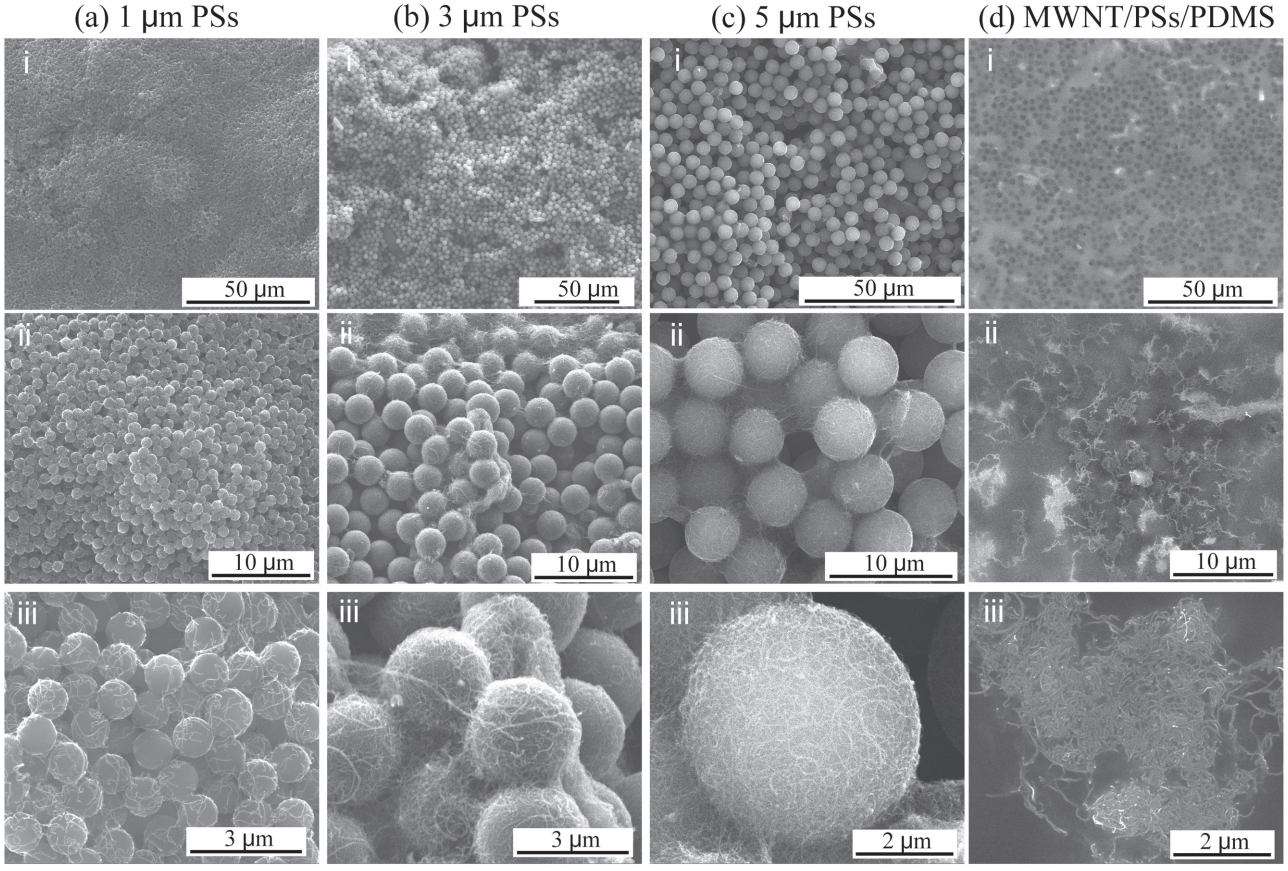

Figure 3. Size of PSs in I-MWNT networks' fabrication. a) 1 μm PSs, b) 3 μm PSs, c) 5 μm PSs with a ratio of 1:1 (PSs: MWNT). MWNTs can effectively wrap onto surface of PSs with all these sizes. d) Surface morphology of MWNT/PSs/PDMS. The exposed MWNTs act as the conductive dots for electrical conductance. Sub-panels (i), (ii), and (iii) show different sizes of view for each item.

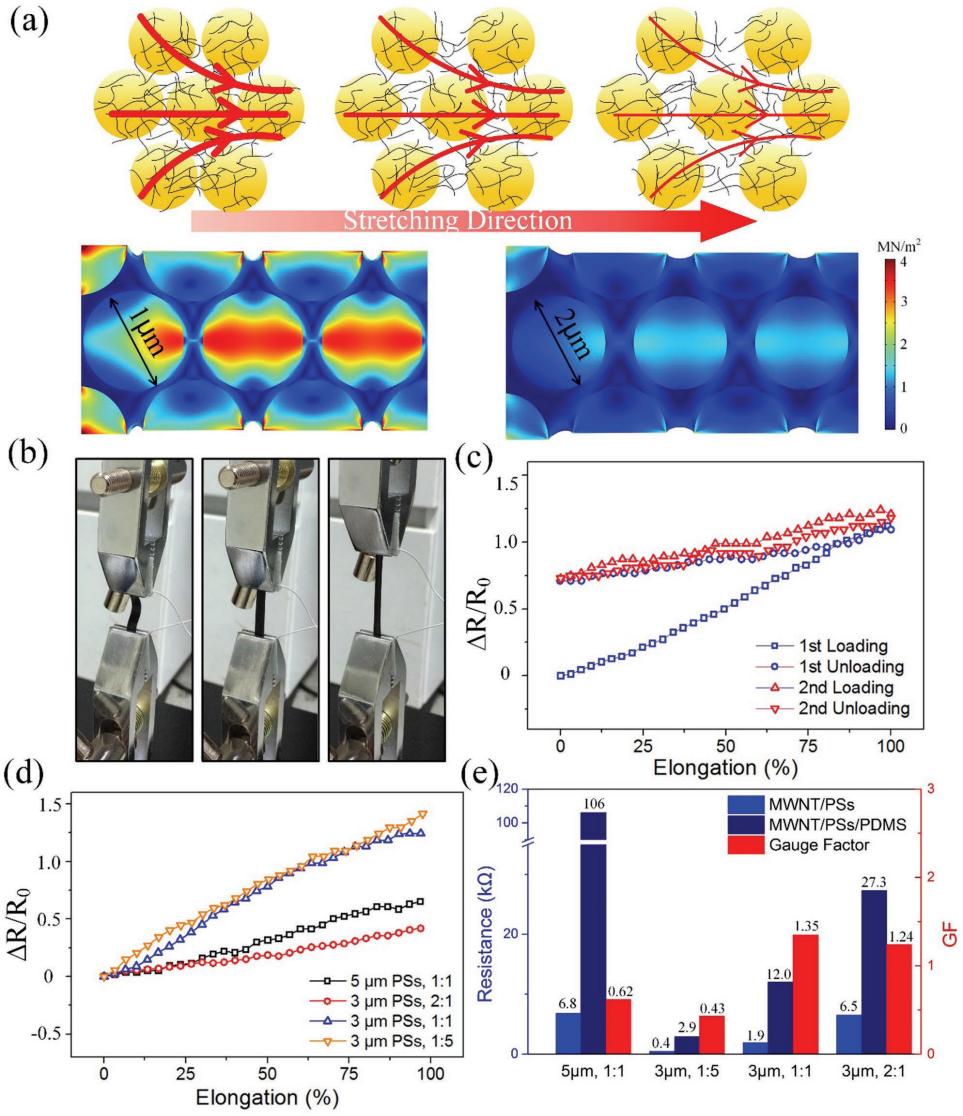

Figure 4. Resistive response during elongation. a) Percolation-based conduction mechanism of MWNT/PSs/PDMS composite. Stretching causes MWNTs losing overlapped area and increases its resistance (Top). Simulation of stress distribution over MWNT/PSs/PDMS composite with different sizes of PSs (1 and 2 μm). Smaller size of PSs leads to larger surface stress under both 10% elongation (Below). b) Loading process by a stretcher and resistance measurement during stretching process. c) Resistive responses of first and second loading and unloading process. d) Resistive responses for different PSs/MWNT recipes at 10th loading process. e) Resistance for MWNT/PSs, MWNT/PSs/PDMS composites and gauge factor for each recipe tested in the experiments.

view, disconnection of overlapped nanomaterials under stretching is caused by the slippage of nanomaterials due to the weak interfacial binding and large stiffness mismatch between nanomaterials and stretchable polymers.[17] In this case, MWNTs connect to each other and maintain its electrical conductance. When the composite is stretched, an applied stress causes the nanotubes to glide from each other, resulting in the increase of electrical resistance. In fact, for MWNT/PSs/PDMS composite, there is another stiffness mismatch between PSs and PDMS, which further enhances the slippage of nanomaterials during stretch. In the strain distribution simulation of PSs/PDMS model shown in Figure 4a, the surface of PS spheres has larger strain than PDMS. At the same time, this phenomenon is more obvious when the size of PSs is smaller as well as its interconnection gaps.

The resistive response of stretchable I-MWNT network sample is tested by a stretcher (Figure 4b). During the elongation test shown, the conductance can be maintained even in high elongation ratio, up to 100%. When we first apply strain onto the membrane, the linear increase of resistance is shown as the 1st loading. The resistance decreases to a lower state at a different pathway when we unload stress for the first time (Figure 4c). The different resistive response between first loading and unloading process can be explained as the reorganization of conductive pathway of MWNT networks.[18,30] After the 1st unloading process, the resistance cannot return to its original state due to residual stress in viscoelastic elastomer. After that process, resistance response can keep stable at a different pathway.

To reveal the electrical characteristics for different recipes, we compare dynamic resistive response during the 10th loading process (Figure 4d) and static resistance difference (Figure 4e) for four different samples. For 3 μm samples (10 mm × 20 mm), the resistance increases gradually with the increase of the amount of MWNT for both MWNT/PSs and MWNT/PSs/PDMS composites. An obvious resistance increase has been observed after the introduction of additional PDMS, which can be explained by the reason that the additional PDMS weakens the connection of MWNTs and the conductance of the networks. This reason can be more significant when the size of PSs becomes larger because larger PSs provides larger space for PDMS to mix with MWNTs. Thus, 5 μm sample of MWNT/PSs/PDMS composite has very high resistance.

Slope of the relative change of the electrical resistance versus applied strain reflects gauge factor of strain gauge. GF is given by $(\Delta R/R_0)/\varepsilon$, where ΔR is the resistance change during stretch, R_0 is the original resistance, ε is the applied strain. When the GFs of different samples are analyzed, samples with smaller size of PSs have larger GF, which can be explained by different strain distributions analyzed in Figure 4a. As the sample without PSs cannot be fabricated successfully by this method, we can discuss the role of PSs in enhancement of gauge factor by comparing sample (1:1) with sample (1:5). For sample (1:5), the increase of resistance can probably be regarded as the disconnection of overlapped MWNTs because the amount of MWNTs is huge (Figure 2c). For sample (1:1), the reason of increase should include the role of PS spheres. The result that sample (1:1) has much higher GF means PSs is responsible for the enhancement of GF.

2.4. Mechanical Durability

The membrane can strongly protect its conductive pathway from external destruction because of its 3D conductive pathway construction. To verify this assumption, the tape test of the sample has been performed and shown in **Figure 5** by comparing with MWNT network directly sprayed onto PDMS surface. Figure 5a shows the experimental results of sprayed MWNT networks before (perfect network connection) and after 10 times tape tests (multiple fractural points), which proves the poor adhesion between sprayed MWNT networks and PDMS surface. However, the images of I-MWNT sample show excellent physical reliability even after 100 times tape tests. The electrical conductance of both samples shown in Figure 5b also proves the results. The resistance of I-MWNT networks barely changes after 100 times of tests, demonstrating that the embedded I-MWNT networks can be self-protected without any further packaging. However, the prayed MWNT networks lose its conductance at its first test, which means it needs to be protected by another sealed layer. PS microspheres and PDMS elastomer help building a safe environment for electrical conductance of MWNT networks, which is superior to completely exposed MWNT networks on PDMS surface by simply sprayed method.

The long time stretching test has also been performed to demonstrate the long-term durability for I-MWNT sample in Figure 5c,d. The result of more than 1000 times test of sample (3 μm PSs, 1:1) shows its remarkable stability. The surface morphology of the sample has no obvious change for sample before stretch after 100th stretch and after 500th stretch, which further proves its mechanical durability over long-term tests.

2.5. Static and Dynamic Gesture Recognition

In **Figure 6**, a dynamic experimental test and a static one have been explored by not only on a single finger of a robot but also attaching onto five fingers of human. For dynamic electrical test, we fixed two ends of one I-MWNT networks sample onto the forefinger of a robot. During bending of forefinger (Figure 6a), the sample is stretched, leading to the increase of electrical resistance. With various bending processes, the resistive response is different accordingly. Figure 6b shows the small and large degree bending processes with slow or fast speeds, and it can be easily distinguished by its dynamic resistive changes. Besides, when the finger bends from small degree to large degree, the resistive response can also be detected. Figure 6c illustrates the change of resistance when the finger bends from 0°, 5°, 18°, 33°, and 55°.

For static detection of resistance and gesture recognition for human beings, five I-MWNT networks samples have been attached on epidermis of five fingers, after which four common hand gestures: half bend of all fingers, "OK," "GREAT," and "YEAH" are performed. When one finger bends, the strain gauge is stretched. By static detection of its original and subsequent resistances, the larger angle the finger bends, the higher resistive change can be detected. The results are illustrated in Figure 6d–f by the resistive change for each finger (left) and the images for each gesture (right), from which the samples can be observed to attach onto fingers conformably. The four gestures performed in our experiments can be distinguished in this way. For instance, with "OK" gesture by hand (Figure 6e), thumb, and forefinger bend and other fingers keep generally straight, which results in great changes of the first and second strain gauges and nearly no change with the others.

3. Conclusion

In summary, we have demonstrated a novel method to fabricate a highly stretchable and robust strain gauge by self-assembly of MWNTs and PS microspheres composites. Different from traditional solvent deposition method, e.g., spraying-coating, the fabrication method protects its conductive pathway by immobilizing MWNT networks in microspheres and PDMS matrix. The gauge factor of the epidermal strain gauge has been proved as 1.35 over more than 1000 times of tests, which is further demonstrated by static and dynamic methods to be sensitive enough for gesture recognition of human fingers.

Analyzed by the SEM photos and electrical results, PSs is regarded to play four dominate roles in this proposed method. First, PS microspheres assist MWNTs to form dense and continuous film in solution evaporation process because of the capillary force in self-assemble of PS microspheres. Second, PS microspheres construct 3D frameworks, which can be occupied by liquid PDMS to form 3D MWNT/PSs/PDMS composite.

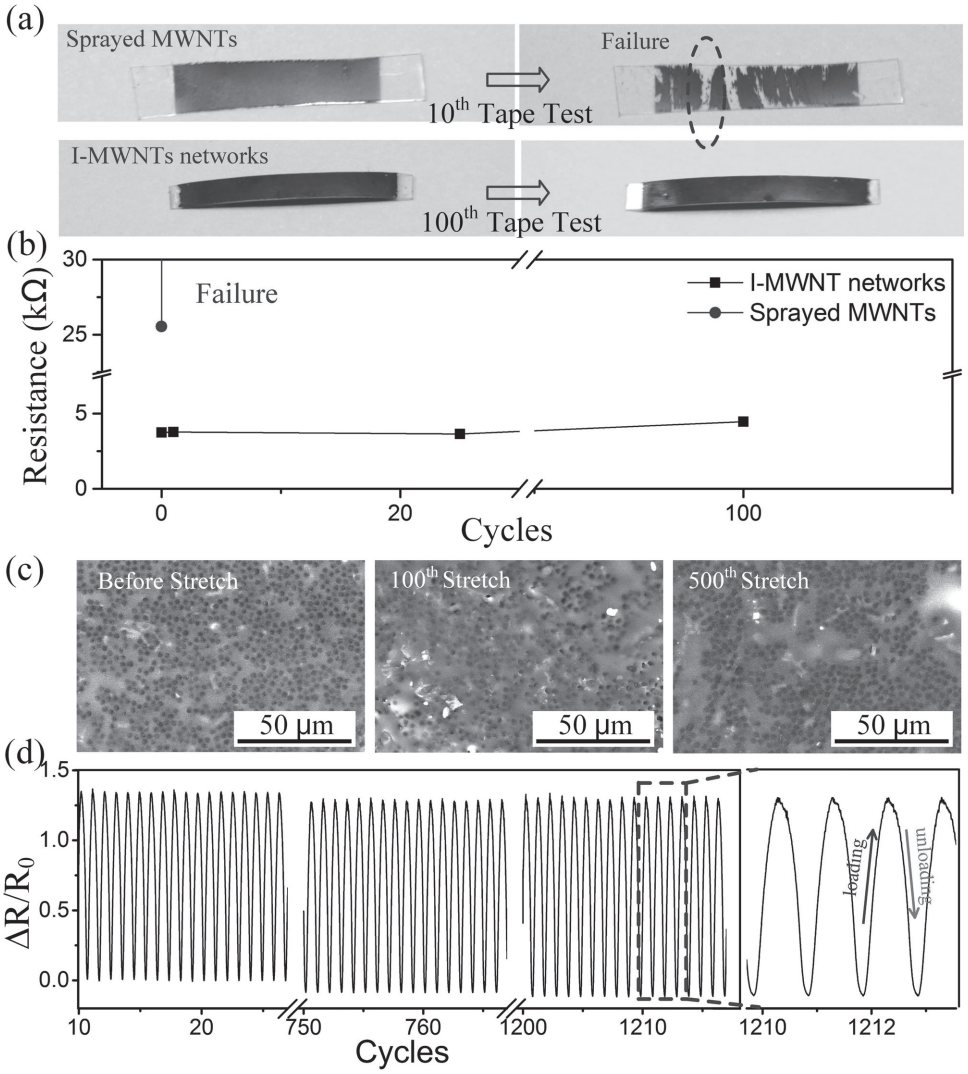

Figure 5. Mechanical durability of I-MWNT networks. a) I-MWNT networks before and after 100 times tape tests compared with a sprayed MWNTs sample. b) Resistance change during tape test. I-MWNT networks can resist damage by tape and its resistance keeps stable, while sprayed MWNT sample fails to conduct at its first test. c) Surface morphologies of MWNT/PSs/PDMS composites before, after 100th and after 500th stretch, respectively. d) Resistive response during long-term elongation (over 1000 times) tests.

Third, PS microspheres alter the stress distribution when the sample is stretched, hence further enhance the gauge factor of the sensor. Last but not least, PS microspheres along with PDMS help protecting MWNTs from the external damage and guarantee its direct use without further packaging after fabrication.

The simple and cost-effective fabrication method, as well as great properties of remarkable elongation ability and mechanical durability, enable this conductive membrane to be a promising strain gauge for actual applications, e.g., in detection of human or robot motions.

4. Experimental Section

Fabrication Process for I-MWNT Networks: First, PS microspheres (1, 3 μm or 5 μm) with a concentration of 10 wt% were suspended in deionized (DI) water, at the same time, MWNTs and the same amount of sodium dodecyl benzene sulfonate (SDBS) were added into DI water (5 mg mL^{-1}). Both suspensions were mixed by ultrasound for three hours, after which the two suspensions were mixed at the ratio of 1:0, 5:1, 2:1, 1:1, 5:1 or 0:1 (PS:MWNT, v:v) and treated by ultrasound for one hour. Then, the mixed suspension was dipped into PDMS mold (20 mm × 10 mm × 0.5 mm) onto glass substrate. The solvent evaporated at 80 °C and left MWNTs and PS microspheres onto the substrate forming the conductive pathway. The thickness of MWNTs and PS arrays can be adjusted by the amount of MWNTs/ PS suspension, which is fixed in our experiment for 100 μL cm^{-2} in our experiments. The liquid PDMS mixture was then solidified at 90 °C for 1 h, after which the composite is gently peeled off from the substrate.

Fabrication Process for Sprayed MWNT Networks: First, the above MWNTs/water suspension was prepared and stored in the spray-coating equipment (HS-08, Vogue Air). Then, PDMS slice was placed onto the hot plate and its temperature was controlled at 200 °C, which is high enough for quick evaporation of sprayed solvent on PDMS surface. The nozzle was placed against PDMS surface with a distance of 10 mm. The spraying speed was controlled at 50 μL s^{-1} and its time duration was 10 min. The sprayed MWNT networks had no further treatment before tape test.

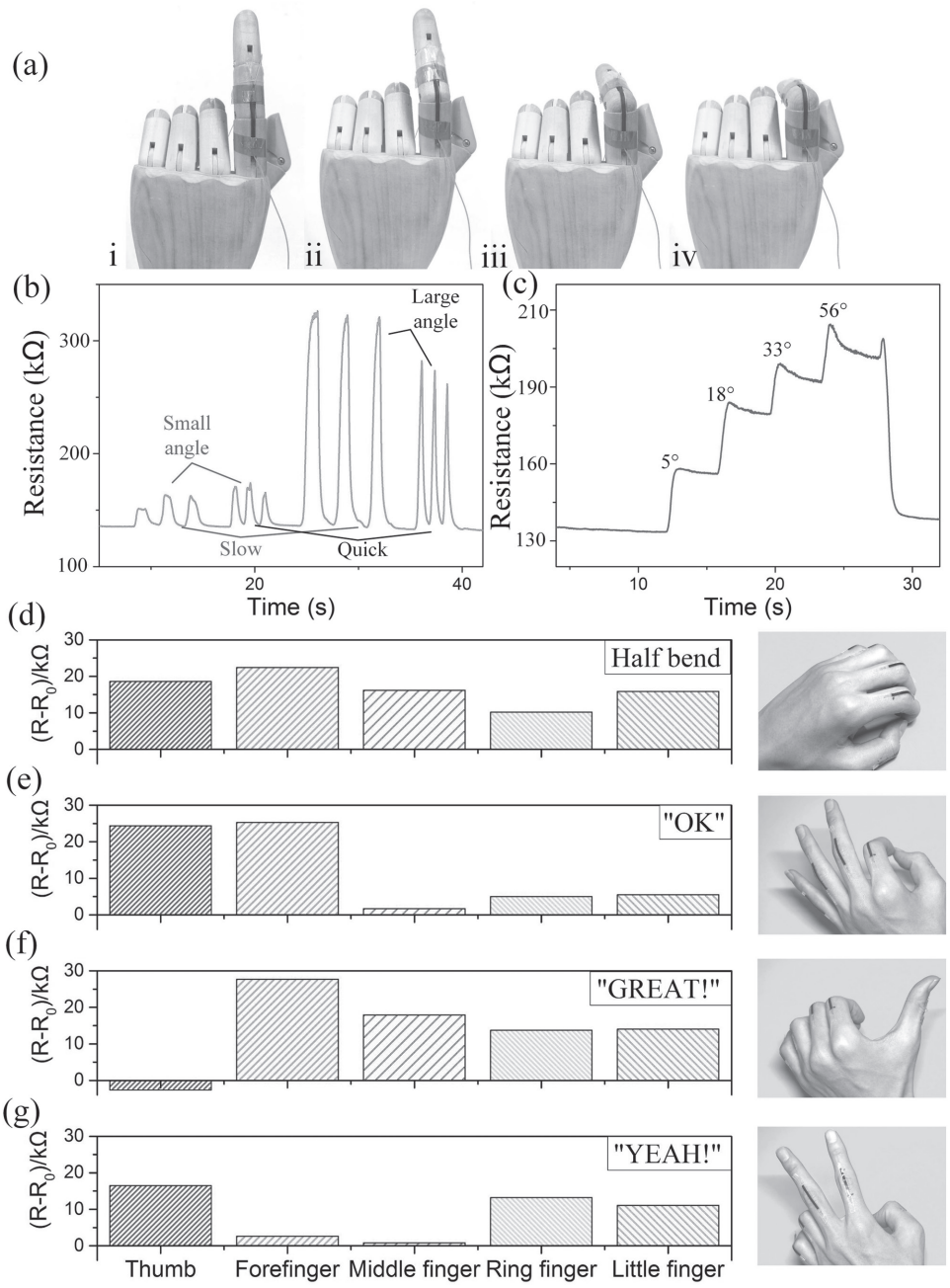

Figure 6. Dynamic and static tests for gesture recognition. a) One sample attached onto forefinger of a robot hand and stretched when the finger bends to different degrees. b) Dynamic resistive response for small and large bending angles at slow and quick bending speeds. c) Dynamic resistive response when bending angle increases from 5° to 56°. Five samples attached onto five fingers and their resistance changes at different gestures: d) half bend of all fingers, e) "OK," f) "GREAT" and g) "YEAH," respectively. Samples are thin enough to be easily attached onto human skins (interconnector lines are not included in the images).

Characterization Setup: The copper interconnector lines were bonded with two ends of the sample by silver paste for good conductivity. The bonding positions were further fixed by 3M or polyimide tape, and then immobilized by two clamps of a tension tester (HSV, HANDPI), which was used to stretch the conductive elastomer to certain position repeatedly. The interconnector lines were then connected to a voltage-stabilized source (MS3050, MAISHENG). The resistance and its change were measured by calculating from direct current detected by low-noise current preamplifier (SR570, SRS) and recorded by a digital oscilloscope (DS1102E, RIGOL). The experiments of gesture recognition are performed in compliance with the relevant laws and institutional guidelines. The institutional committee and the human subject have approved the experiments.

Supporting Information

Supporting Information is available from the Wiley Online Library or from the author.

Acknowledgements

This work was supported by the National Natural Science Foundation of China (Grant Nos. 61674004 and 91323304), National Key Research and Development Program of China (Grant No. 2016YFA0202701), and the Beijing Science & Technology Project (Grant No. D151100003315003) and the Beijing Natural Science Foundation of China (Grant No. 4141002).

Conflict of Interest

The authors declare no conflict of interest.

Keywords

epidermal sensors, gesture recognition, percolation networks, self-assembly

Received: June 21, 2017
Revised: August 11, 2017
Published online: November 2, 2017

[1] S. Wagner, S. Bauer, *MRS Bull.* **2012**, *37*, 207.
[2] S. Gong, W. Cheng, *Adv. Electron. Mater.* **2017**, *3*, 1600314.
[3] X. Li, L. Zhang, X. Wang, I. Shimoyama, X. Sun, W.-S. Seo, H. Dai, *J. Am. Chem. Soc.* **2007**, *129*, 4890.
[4] S. J. Benight, C. Wang, J. B. H. Tok, Z. Bao, *Prog. Polym. Sci.* **2013**, *38*, 1961.
[5] L. Cai, J. Li, P. Luan, H. Dong, D. Zhao, Q. Zhang, X. Zhang, M. Tu, Q. Zeng, W. Zhou, S. Xie, *Adv. Funct. Mater.* **2012**, *22*, 5238.
[6] M. L. Hammock, A. Chortos, B. C. K. Tee, J. B. H. Tok, Z. A. Bao, *Adv. Mater.* **2013**, *25*, 5997.
[7] H. L. Filiatrault, G. C. Porteous, R. S. Carmichael, G. J. E. Davidson, T. B. Carmichael, *Adv. Mater.* **2012**, *24*, 2673.
[8] C. Keplinger, J. Sun, C. C. Foo, P. Rothemund, G. M. Whitesides, Z. Suo, *Science* **2013**, *341*, 984.
[9] D. Son, J. Lee, S. Qiao, R. Ghaffari, J. Kim, J. E. Lee, C. Song, S. J. Kim, D. J. Lee, S. W. Jun, *Nat. Nanotechnol.* **2014**, *9*, 397.
[10] D. H. Kim, N. S. Lu, R. Ma, Y. S. Kim, R. H. Kim, S. D. Wang, J. Wu, S. M. Won, H. Tao, A. Islam, K. J. Yu, T. I. Kim, R. Chowdhury, M. Ying, L. Xu, M. Li, H. J. Chung, H. Keum, M. McCormick, P. Liu, Y. W. Zhang, F. G. Omenetto, Y. G. Huang, T. Coleman, J. A. Rogers, *Science* **2011**, *333*, 838.
[11] S. H. Jeong, S. Zhang, K. Hjort, J. Hilborn, Z. Wu, *Adv. Mater.* **2016**, *28*, 5830.
[12] X. Huang, Y. Liu, K. Chen, W.-J. Shin, C.-J. Lu, G.-W. Kong, D. Patnaik, S.-H. Lee, J. Fajardo Cortes, J. A. Rogers, *Small* **2014**, *10*, 3083.
[13] D. Qi, Z. Liu, M. Yu, Y. Liu, Y. Tang, J. Lv, Y. Li, J. Wei, B. Liedberg, Z. Yu, X. Chen, *Adv. Mater.* **2015**, *27*, 3145.
[14] Z. Y. Liu, M. Yu, J. H. Lv, Y. C. Li, Z. Yu, *ACS Appl. Mater. Interfaces* **2014**, *6*, 13487.
[15] S. Rosset, H. Shea, *Appl. Phys. A* **2013**, *110*, 281.
[16] Z. Su, X. Chen, H. Chen, Y. Song, X. Cheng, B. Meng, Z. Song, H. Zhang, *2017 IEEE 30th Int. Conf. on IEEE on Micro Electro Mechanical Systems (MEMS)*, IEEE, Las Vegas, NV, USA **2017**, p. 1036.
[17] M. Amjadi, K. U. Kyung, I. Park, M. Sitti, *Adv. Funct. Mater.* **2016**, *26*, 1678.
[18] F. Xu, Y. Zhu, *Adv. Mater.* **2012**, *24*, 5117.
[19] K. K. Kim, S. Hong, H. M. Cho, J. Lee, Y. D. Suh, J. Ham, S. H. Co, *Nano Lett.* **2015**, *15*, 5240.
[20] N. N. Jason, M. D. Ho, W. Cheng, *J. Mater. Chem. C* **2017**, *5*, 5845.
[21] P. Lee, J. Lee, H. Lee, J. Yeo, S. Hong, K. H. Nam, D. Lee, S. S. Lee, S. H. Ko, *Adv. Mater.* **2012**, *24*, 3326.
[22] T. Sekitani, H. Nakajima, H. Maeda, T. Fukushima, T. Aida, K. Hata, T. Someya, *Nat. Mater.* **2009**, *8*, 494.
[23] L. Hu, D. S. Hecht, G. Grüner, *Nano Lett.* **2004**, *4*, 2513.
[24] M. C. LeMieux, M. Roberts, S. Barman, Y. W. Jin, J. M. Kim, Z. N. Bao, *Science* **2008**, *321*, 101.
[25] D. J. Lipomi, B. C. K. Tee, M. Vosgueritchian, Z. N. Bao, *Adv. Mater.* **2011**, *23*, 1771.
[26] W. R. Small, M. I. H. Panhuis, *Small* **2007**, *3*, 1500.
[27] M. Amjadi, A. Pichitpajongkit, S. Lee, S. Ryu, I. Park, *ACS Nano* **2014**, *8*, 5154.
[28] M. Giersig, P. Mulvaney, *Langmuir* **1993**, *9*, 3408.
[29] M. Park, J. Park, U. Jeong, *Nano Today* **2014**, *9*, 244.
[30] F. Xu, X. Wang, Y. Zhu, Y. Zhu, *Adv. Funct. Mater.* **2012**, *22*, 1279.

